Supporting Information

Engineering the Composition and Crystallinity of Molybdenum Sulfide for High-performance Electrocatalytic Hydrogen Evolution

Yanpeng Li[1,2§]*, Yifei Yu[2§], Robert A. Nielsen[3], William A. Goddard III[3], Yao Li[1], Linyou Cao[2,4]*

[1]Center for Composite Materials and Structures, Harbin Institute of Technology, Harbin Heilongjiang 150001, China; [2]Department of Materials Science and Engineering, North Carolina State University, Raleigh NC 27695, USA;
[3] Materials and Process Simulation Center, California Institute of Technology, Pasadena CA 91125, USA; [4]Department of Physics, North Carolina State University, Raleigh NC 27695, USA;

[§]These authors contribute equally.

*To whom the correspondence should be addressed:

yanpengli@hit.edu.cn and lcao2@ncsu.edu

This PDF file includes

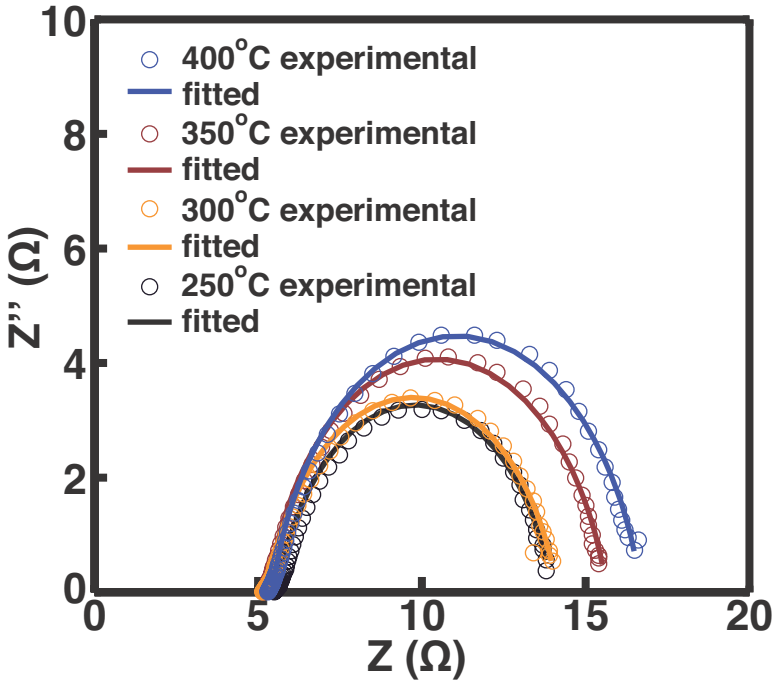

Figure S1. Electrochemical impedance spectrocopies of molybdenum sulfide materials grown at different temperatures. The experimental results (circles) are fitted by using an equivalent Randles circuit model was fit to the data with ZSimpWin software. The growth temperature is given as shown.

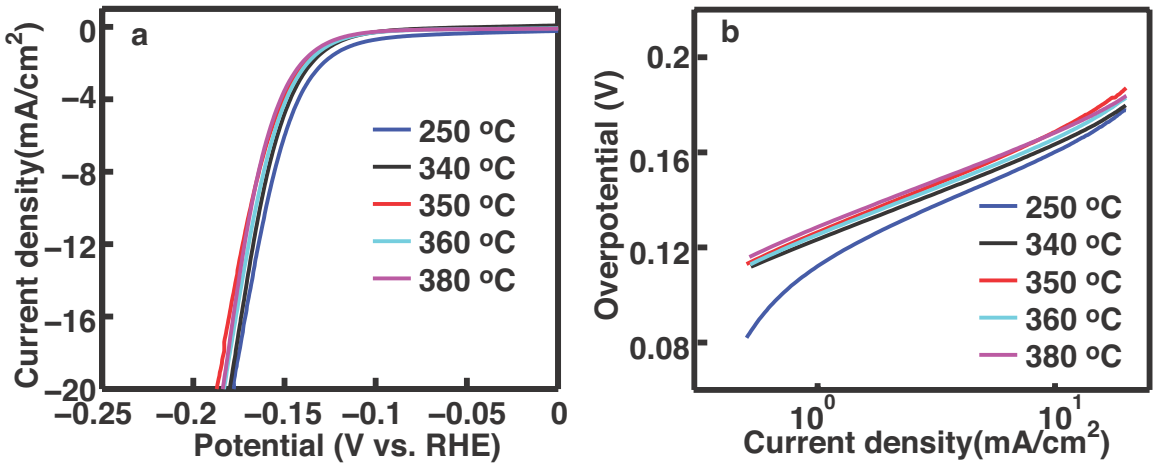

Figure S2. (a) Polarization curves and (d) Tafel plots of the molybdenum sulfide materials grown at different temperatures as indicated.

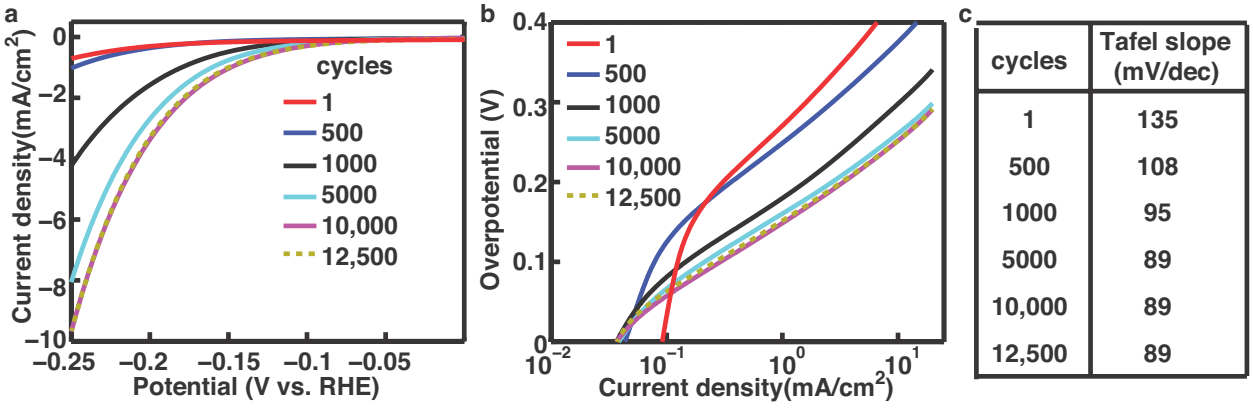

c

cycles	Tafel slope (mV/dec)
1	135
500	108
1000	95
5000	89
10,000	89
12,500	89

Figure S3. Improvement in the catalytic activities of molybdenum sulfide materials grown at 550°C with scanning cycles. (a) Polarization curves and (d) Tafel plots of the molybdenum sulfide materials at different cycles. (c) Tabulated Tafel slopes at the different cycles derived from (b).

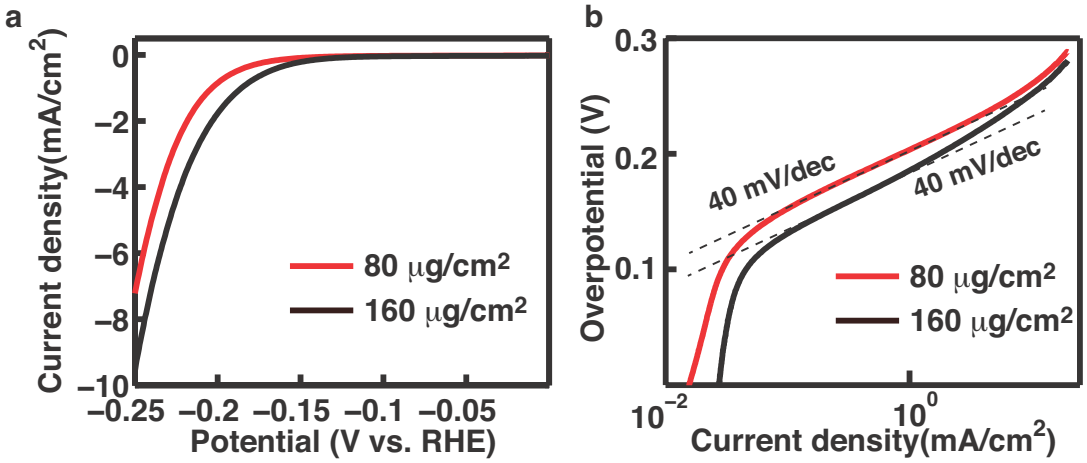

Figure S4. (a) Polarization curves and (d) Tafel plots of the molybdenum sulfide materials grown at the same temperatures (350°C) but with different loadings as indicated.

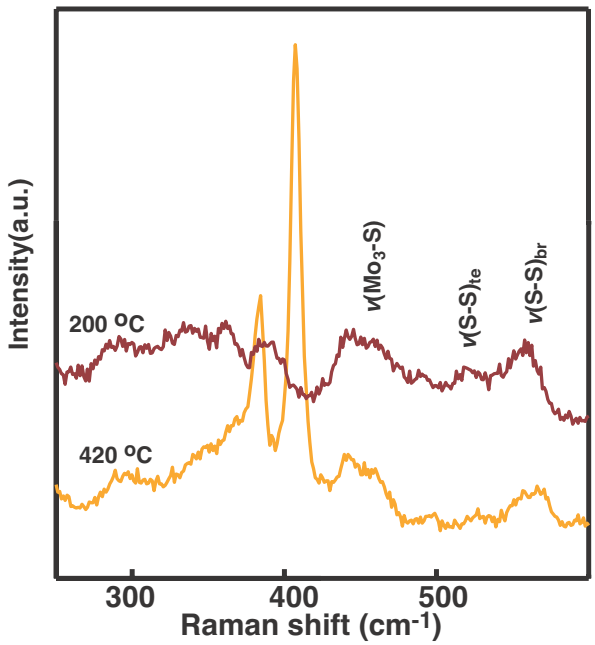

Figure S5. Raman spectra of the molybdenum sulfide materials grown at 200°C and 420°C. This is to show the existence of MoS_3 peaks in the materials grown at 420 °C.

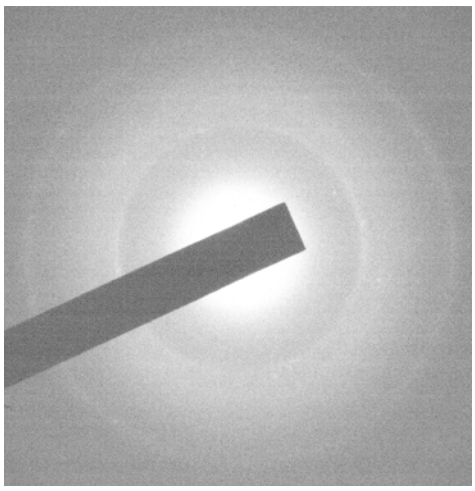

Figure S6. Typical electron diffraction pattern collected from the molybdenum sulfide materials grown at 400°C.

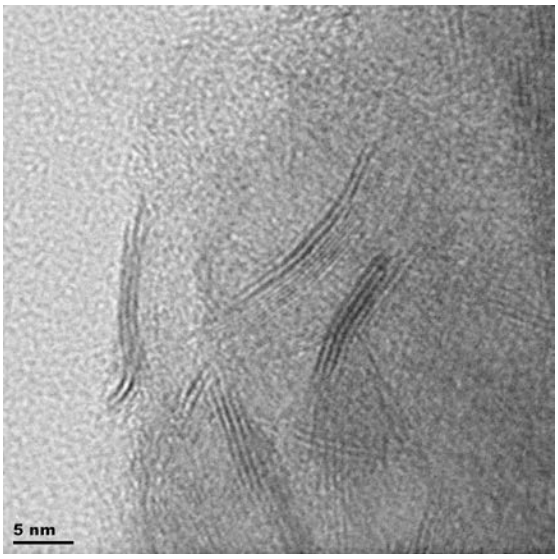

Figure S7. Typical TEM image of the molybdenum sulfide materials grown at 420°C.

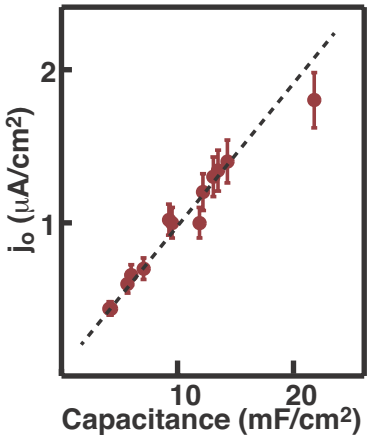

Figure S8. Exchange current densities of the molybdenum sulfide grown at the low temperatures as a function of the capacitance of the materials. The different capacitance indicates the surface area of the materials and was mainly controlled by using substrates with different roughness. For example, the materials with low capacitance were grown on glassy carbon and those with relatively high capacitance were grown on graphite substrates. We have confirmed that the synthesized film is typically thick enough to prevent the influence from the substrate other than enabling different surface areas. The dashed line is to schematically illustrate the linear correlation between the exchange current density and the surface area.

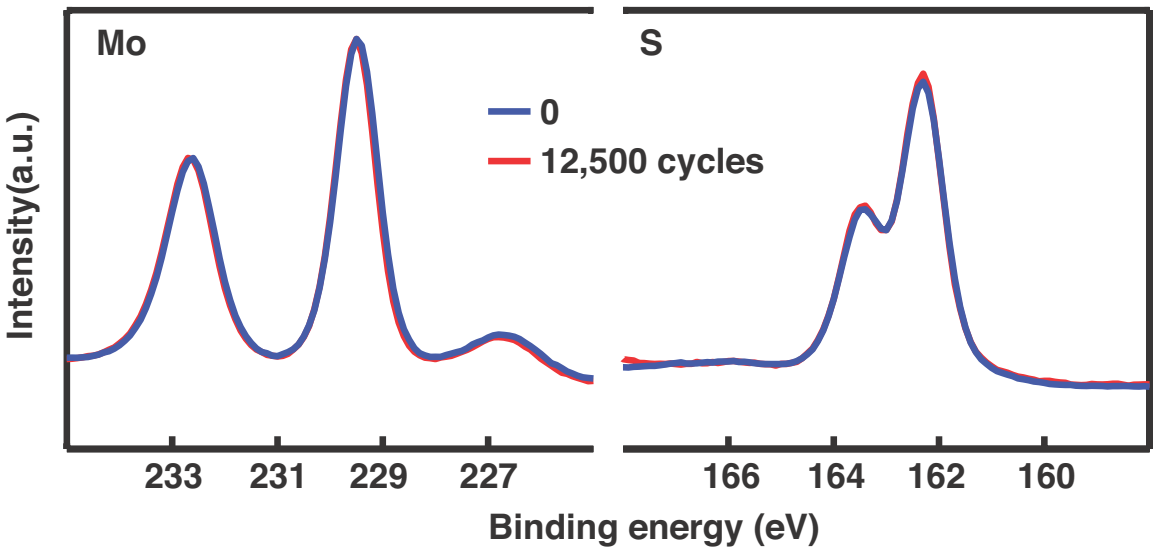

Figure S9. XPS spectra of the molybdenum sulfide materials grown at 600°C with different scanning cycles.

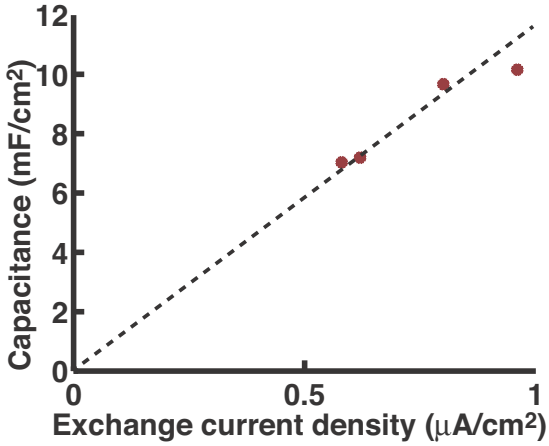

Figure S10. The capacitance and exchange current density collected from the molybdenum sulfide materials grown at 300°C during the continuous CV process. The number of the cycles when the results were collected are 250, 500, 1000, and 2000 from the highest to the lowest exchange current densities, respectively.

Density Functional Theory Calculations

In order to help interpret the experimental results we carried out Density Functional Theory (DFT) calculations (M06L)[1] within the PBF Poisson-Boltzmann continuum solvation model[2] to determine the structure and properties of MoS_3 and low-crystallinity MoS_2 materials as a function of net charge and state of protonation. Because MoS_3 bear similar XPS and Raman results as MoS_3[3,4], we consider it it can be used as a computation model for our studies.

Structures and Electronic energies of the species in this study were calculated using density functional theory. The structures were first optimized using the B3LYP flavor of DFT with the LACVP** core effective potential and basis set. This was further refined using the M06L flavor of DFT using LACV3P**++ basis set on molybdenum atom and 6-311++G-3df-3pd basis set on sulfur atom. We use the M06L functional because the relative electronic energies agree with the results in periodic plane wave calculations[1]. The Vibrational frequencies were calculated for the optimized structures to obtain zero point energies, entropies, and enthalpies at room temperature. Solvation energies were calculated using the PBF (Jaguar) Poisson-Boltzmann polarizable continuum method using a dielectric constant of 80.37 and a probe radius at 1.4 Å for liquid water. The final Gibbs free energy for each species is the sum of electronic energy, vibrational energies, and solvation energy:

$$G = E + ZPE + H_{\text{vib}} - TS_{\text{vib}} + G_{\text{sol}}$$

Where G is the Gibbs free energy, E is the electronic energy, ZPE is the zero point energy, H_{vib} and S_{vib} are the vibrational enthalpy and entropy, G_{sol} is the solvation energy.

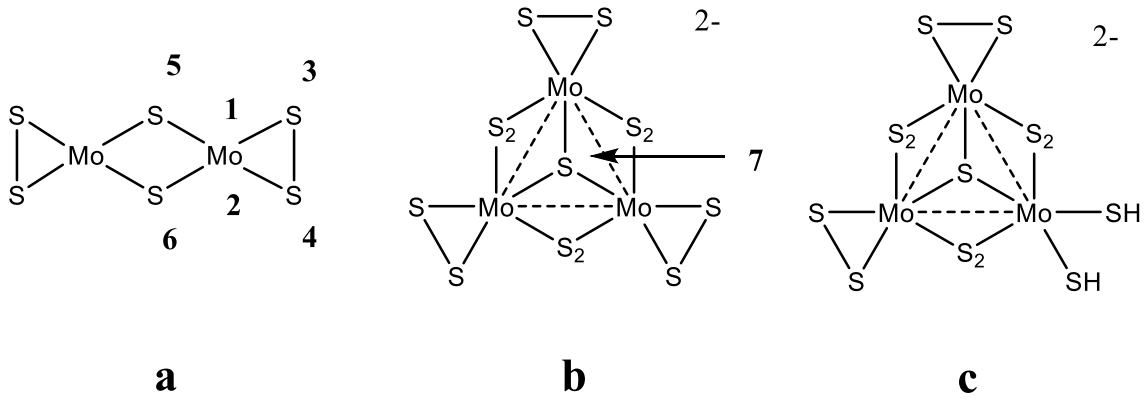

Fig S10. Hydrogen adsorption sites on the $Mo_3S_{13}^{2-}$ cluster. (**a**) Possible sites are the molybdenum atom, the bridging sulfur atoms, and the terminal sulfur atoms. The structure is oriented with the apical sulfur on top. (**b**) Hydrogen adsorption site on the apical sulfur atom. (**c**) Two hydrogen atoms bound to the terminal sulfur atoms.

Results & Discussion

Our calculations indicate that the active catalytic site for HER in amorphous molybdenum sulfide is the terminal sulfur. We find many adsorption sites for hydrogen atoms on the $Mo_3S_{13}^{2-}$ cluster. The adsorption energies on the top (site **1**) and bottom (site **2**) Mo atoms are 50.86 kcal/mol and 43.36 kcal/mol from the resting state, indicating that Mo-H species are not involved in an intermediate step. The reason for this unfavorable energy is that the molybdenum atom is

already 7 coordinated, making it energetically costly to add another hydrogen to the atom. It is likely that this is the same case in the amorphous MoS_3 materials. Thus we consider only H bonded to S.There are three kinds of sulfur atoms in the cluster. We believe that the apical sulfur (site **7**) behave chemically like the bulk sulfurs in the basal plane of crystalline MoS_2 because they share the same coordination environment. The calculated hydrogen adsorption energy on the apical sulfur is 41.66 kcal/mol, which makes adsorption of hydrogen at this site prohibitive. The adsorption energies on the bridging and terminal sulfur atoms are relatively favorable. They are 22.23 kcal/mol for the top (site **3**) and 17.49 kcal/mol bottom (site **4**) of the terminal sulfurs and 17.18 kcal/mol for the top (site **5**) and 22.66 kcal/mol bottom (site **6**) bridging sulfurs. Since both types of sulfur atoms involve a S-S dimer the dimer S-S bond must break, as the H is bonded, making the site less favorable.

Since all of the above single site adsorption energies are very high, we conclude that none of these structures are involved in immediate steps for hydrogen evolution. The alternative, is a concerted reaction in which hydrogen atoms are adsorbed in pairs. Thus adding two hydrogen atoms to the terminal sulfurs to form structure c, leads to a the free energy of -6.5 kcal/mol downhill from the $Mo_3S_{13}^{2-}$ structure. This indicates that the reaction free energy for H_2 formation is only 6.5 kcal/mol, making it a plausible pathway for hydrogen evolution. However such a 2s+2s reaction to form H_2 is symmetry prohibited (Woodward-Hoffmann rule). However in the presence of water solvent, a water molecule bridging the two S-H groups can serve as a catalyst to form H_2. In this case one H of the bridging water combines with the H on one SH group to form H2, while the H on the other SH group transfers to the water, leaving the water intact. This can lower the reaction barrier substantially.

If the barrier for H_2 formation is in the same order as the reaction energy of 6.5 kcal/mol, the rate of electron transfer can be important. This may explain the 40 mV/dec Tafel slope observed here and previously in[2]. In this case the reactions takes place with one electron reduction as a pre-equilibrium step, and the second reduction as the rate-determining step, resulting in 60/(1+0.5)=40 mV/dec. Of course the 40mV/dec could also be due to other effects, for example, two competing reactions with an average Tafel slope of 40mV/dec. However since the new mechanism with Tafel slope of 40mV/dec is observed to turn on for materials prepared in decreasing temperatures, we considering that an averaging effect is unlikely.

References

(1) Zhao, Y.; Truhlar, D. G. *J. Chem. Phys.* **2006**, *125*.

(2) Tannor, D. J.; Marten, B.; Murphy, R.; Friesner, R. A.; Sitkoff, D.; Nicholls, A.; Ringnalda, M.; Goddard, W. A.; Honig, B. *J. Am. Chem. Soc.* **1994**, *116*, 11875.

(3) Kibsgaard, J.; Jaramillo, T. F.; Besenbacher, F. *Nat. Chem.* **2014**, *6*, 248.

(4) Weber, T.; Muijsers, J. C.; Niemantsverdriet, J. W. *J. Phys. Chem.* **1995**, *99*, 9194.